Distinct potassium channels on pain-sensing neurons

Matthew N. Rasband*, Eunice W. Park*, Todd W. Vanderah†, Josephine Lai†, Frank Porreca†, and James S. Trimmer*‡

*Department of Biochemistry and Cell Biology, State University of New York, Stony Brook, NY 11794; and †Department of Pharmacology, University of Arizona Health Sciences Center, Tucson, AZ 85724

Edited by Lily Y. Jan, University of California, San Francisco, CA, and approved September 5, 2001 (received for review July 19, 2001)

Differential expression of ion channels contributes functional diversity to sensory neuron signaling. We find nerve injury induced by the Chung model of neuropathic pain leads to striking reductions in voltage-gated K^+ (Kv) channel subunit expression in dorsal root ganglia (DRG) neurons, suggesting a potential molecular mechanism for hyperexcitability of injured nerves. Moreover, specific classes of DRG neurons express distinct Kv channel subunit combinations. Importantly, Kv1.4 is the sole Kv1 α subunit expressed in smaller diameter neurons, suggesting that homomeric Kv1.4 channels predominate in Aδ and C fibers arising from these cells. These neurons are presumably nociceptors, because they also express the VR-1 capsaicin receptor, calcitonin gene-related peptide, and/or Na^+ channel SNS/PN3/Nav1.8. In contrast, larger diameter neurons associated with mechanoreception and proprioception express high levels of Kv1.1 and Kv1.2 without Kv1.4 or other Kv1 α subunits, suggesting that heteromers of these subunits predominate on large, myelinated afferent axons that extend from these cells.

In the peripheral nervous system (PNS), sensory neuron cell bodies reside in dorsal root ganglia (DRG), and extend axons that innervate both peripheral and central targets. A diverse group of ligand- and voltage-gated ion channels transduce innocuous and noxious (nociceptive) stimuli into depolarizations that are conducted along axons and finally converted into neurotransmitter release. For example, nociceptive neurons express specific ion channels [ATP-gated channels, voltage-gated Na^+ channels (NaChs), H^+-gated channels, and capsaicin receptor channels] that represent attractive targets for therapeutic intervention of peripheral pain (1). Little is known of the molecular identity of the voltage-gated K^+ (Kv) channels that regulate membrane repolarization, resting membrane potential, frequency of firing, and neurotransmitter release in sensory neurons. Mammalian *Shaker*-related or Kv1 proteins are composed of four transmembrane α subunits (2–4), and up to four modulatory cytoplasmic Kvβ subunits (5, 6).

The predominant Kv1 channels in myelinated nerve fibers comprise coassembled Kv1.1, Kv1.2, and Kvβ2.1 (7–9) that would form dendrotoxin (DTX)-sensitive delayed-rectifier channels as Kv1.1, Kv1.2 and Kv1.6 are DTX-sensitive. DTX-sensitive transient or A-type channels in unmyelinated axons of many central neurons consist of Kv1.1 and/or Kv1.2 coassembled with Kv1.4 (10–12). Distinct populations of defined DRG neurons express a variety of Kv currents whose pharmacological blockade affects neuronal excitability (13–16). Nerve injury results in reductions in Kv currents, hyperexcitability, and hyperalgesia (17). To better understand the molecular physiology and pharmacology of sensory neurons, and to identify specific Kv channels that may represent potential targets for therapeutics to treat peripheral pain, we investigated Kv1 subunit expression in mammalian DRG before and after nerve injury.

Materials and Methods

Antibodies. Antibodies against Kv subunits (8, 11, 18, 19) and the pan-NaCh antibody (20) have been described. The Nav1.8 and VR-1 antibodies were kind gifts from S. R. Levinson (Univ. of Colorado Health Sciences Center, Denver) and S. Haleguoa (State Univ. of New York, Stony Brook), respectively. The anti-calcitonin gene-related peptide (CGRP) and Neurofilament-M (NF-M) antibodies were purchased from Peninsula Laboratories and Chemicon, respectively. Preincubation of antibodies with a molar excess of the antigen used to generate the antibody eliminated all tissue staining (data not shown).

Immunofluorescence. DRG (L4-L6) from adult rats (>4 months old) were dissected, immediately fixed in ice cold 4% paraformaldehyde in 0.1 M phosphate buffer (PB), pH 7.2, for 30 min, transferred to ice-cold 20% sucrose solution in 0.1 M PB until equilibrated, and then frozen in Tissue-Tek (Miles, Elkhart, IL) OCT mounting medium. Sections were cut, placed in 0.1 M PB, spread on gelatin coated coverslips, and allowed to air dry. For staining of rat bladder, the bladder was dissected and immersed in Locke's solution (in mM: NaCl 154, KCl 5.6, $CaCl_2$ 2, Hepes 10, pH 7.4), cut at the midline, and the muscle layer separated from the urothelium. These two distinct layers were then fixed in 4% paraformaldehyde in 0.1 M PB for 30 min, cut into small pieces, placed on glass coverslips, and air dried. Immunofluorescence staining was performed as described (21). Secondary antibodies were Alexa 488-conjugated goat anti-rabbit or anti-guinea pig, and Alexa 594-conjugated goat anti-mouse or goat anti-rabbit antibodies (Molecular Probes). For triple-labeling experiments, the anti-mouse secondary antibodies were Alexa 350 anti-IgG_{2b} and tetramethylrhodamine B isothiocyanate (TRITC) conjugated anti-IgG_1 (Southern Biotechnology Associates). Digital images were collected on a Zeiss Axioskop 2 fluorescence microscope fitted with either a SPOT or an Axiocam color CCD camera, and analyzed by using PHOTOSHOP (Adobe Systems, Mountain View, CA) or NIH IMAGE software.

Injury Model. Male Sprague–Dawley rats were maintained in a climate-controlled room on a 12-h light/dark cycle and food and water were available *ad libitum*. All testing was performed in accordance with policies and recommendations of the International Association for the Study of Pain and the National Institutes of Health guidelines for handling and use of laboratory animals and received approval from the Institutional Animal Care and Use Committee of the University of Arizona. Spinal nerve ligation (SNL) injury was induced by using the procedure of Kim and Chung (22). Anesthesia was induced with 2% halothane in O_2 at 2 l/min and maintained with 0.5% halothane in O_2. After surgical preparation of rats and exposure of dorsal vertebral column from L4 to S2, the L5 and L6 spinal nerves were tightly ligated distal to the DRG. The incision was closed and the animals were allowed to recover for 7–9 days. Rats that exhibited motor deficiency (such as paw-dragging) or failure to exhibit subsequent tactile allodynia were excluded from further testing (less than 5%). Sham control rats underwent the same

This paper was submitted directly (Track II) to the PNAS office.

Abbreviations: DRG, dorsal root ganglia; CGRP, calcitonin gene-related peptide; Kv, voltage-gated K^+; NaChs, voltage-gated Na^+ channels; DTX, dendrotoxin; NF-M, Neurofilament-M.

‡To whom reprint requests should be addressed at: Department of Biochemistry, State University of New York, Stony Brook, NY 11794-5215. E-mail: james.trimmer@sunysb.edu.

The publication costs of this article were defrayed in part by page charge payment. This article must therefore be hereby marked "*advertisement*" in accordance with 18 U.S.C. §1734 solely to indicate this fact.

Table 1. Quantitative analysis of Kv channel expression

Reference antibody	Incidence, % (*n*)*						Average diameter, μm†	ipsi/contra‡
	Kv1.1	Kv1.2	Kvβ2.1	Kv1.4	Nach	VR-1		
Kv1.1	—	92 (134)	76 (84)	28 (53)	6 (141)	ND	38.0 ± 9	0.49
Kv1.2	100 (123)	—	91 (284)	18 (282)	19 (181)	ND	33.0 ± 11	0.36
Kvβ2.1	100 (58)	93 (226)	—	69 (157)	ND	ND	36.0 ± 10	0.75
Kv1.4	15 (101)	20 (221)	38 (283)	—	93 (364)	ND	26.5 ± 10	0.40
NaCh	2 (369)	11 (327)	ND	88 (401)	—	60 (349)	26.2 ± 8	0.18
VR-1	ND	ND	ND	ND	73 (259)	—	18.1 ± 5	0.13

*Incidence of double-labeling of reference antibody (left column) versus each of the antibodies used in this study (rows). For example, 92% of the Kv1.1-positive cells also expressed Kv1.2, whereas 100% of the Kv1.2-positive cells also expressed Kv1.1. ND, not determined.
†Average cell diameter of immunoreactive cells, $n \geq 200$ cells per sample.
‡Ratio of fluorescence intensity from ipsilateral L5/L6 injured DRG to contralateral L5/L6 DRG. Ratio for NF-M control was 0.96.

operation and handling as experimental animals, but without SNL.

Quantitation. Positively labeled cells from randomly selected DRG sections were identified by manually selecting a threshold above which cells were clearly labeled, after which diameters of individually labeled neurons where the nucleus was clearly identified were measured in Adobe PHOTOSHOP. To avoid counting and measuring cells more than once each cell was tagged after measurement. Intensities of labeled cells or regions were measured by using NIH IMAGE. For ratios of fluorescence intensity between the ipsi- and contralateral DRG from the injury model, ten positively labeled neurons from the contralateral DRG were measured for average fluorescence intensity. Because ipsilateral DRG neurons all had very low fluorescence intensities, and because cells that before the injury had been labeled positively for a particular ion channel could not be identified, large areas containing many (>50) cells were measured and an average fluorescence intensity for the entire area calculated. Only in the case of the Kvβ2.1 and the NF-M-labeled cells could the outline of individual cells be identified. In all cases where images of ipsi- and contralateral DRG were compared, sections were stained side by side, and unless otherwise noted, all reagents and imaging parameters were identical.

Results

Kv1 Subunit Expression Is Altered in Injured DRG. Because neuronal excitability can be affected dramatically by changes in ion channel expression, we tested whether Kv1 channel expression in mammalian DRG was altered by nerve injury. We used an established model of neuropathic pain in which spinal nerves corresponding to L5 and L6 were tightly ligated distal to the DRG, but those afferent fibers deriving from L4 were undamaged (22). In contrast to contralateral DRG, injury resulted in >50% reduction in the level of Kv1 α subunit expression in ipsilateral L5/L6 DRG (Fig. 1 , Table 1), whereas there was little change in uninjured ipsilateral L4 DRG (Fig. 1). Further, overall expression of both NaChs and VR-1 was reduced by 80–90% in injured DRG (Fig. 1, Table 1). In contrast to these ion channels, NF-M immunoreactivity in the injured DRG was unchanged relative to the contralateral control (Fig. 1; ratio of ipsilateral fluorescence intensity to contralateral fluorescence intensity = 0.96), indicating that the DRG neurons were viable and that the observed reduction in ion channel expression was specific. In contrast to the dramatic reduction in Kv1 α subunit expression, Kvβ2.1 expression was reduced by only 25%, suggesting a potential role for Kvβ2.1 independent of its association with Kv1 channels (23).

Kv1 Subunit Expression Varies in Different DRG Neurons. In uninjured DRG only a subset of Kv1 α subunits were expressed, and expression varied between distinct classes of neurons. Kv1.1 and Kv1.2 were expressed primarily in larger-diameter neurons (Fig. 2, arrowheads; Table 1). In contrast, Kv1.4 was mainly expressed in smaller-diameter cells (Fig. 2, arrow; Table 1), as well as rare larger-diameter neurons (Fig. 2, asterisk). Within the individual cell bodies, Kv1 subunit staining was present uniformly throughout the cytoplasm, presumably representing recently synthesized populations in the endomembrane system. We found that among Kvβ subunits, only Kvβ2.1 was detected and was most abundant in larger diameter cells (Fig. 1, Table 1). Anti-Kv1.3, Kv1.5, Kvβ1.1, and Kvβ1.2 antibodies did not react with DRG sections or with immunoblots of crude rat DRG membranes, and Kv1.6 was detected at very low levels only on immunoblots (see Figs. 5–7, which are published as supporting information on the PNAS web site, www.pnas.org). Thus, the delayed-rectifier channel subunits Kv1.1 and Kv1.2, with Kvβ2.1, predominate in large-diameter neurons, and the A-type channel subunit Kv1.4 in small-diameter neurons.

We used specific immunohistological markers and measurement of neuronal cell body diameter to correlate Kv1 subunit expression with functional classes of DRG neurons (Fig. 1). The large-diameter neurons expressing Kv1.1, Kv1.2, and Kvβ2.1 (Figs. 1 and 2) likely correspond to the Aα and Aβ myelinated afferent fibers. Although all neurons express NaChs, pan-NaCh staining revealed a distinct subpopulation of small diameter cells (26 ± 8 μm) that had the greatest NaCh density. Importantly, both the average diameter and the distribution of diameters of these cells were nearly identical to Kv1.4-expressing cells (Fig. 2, Table 1). The thermal receptor VR-1 (24) was also expressed at high levels in small-diameter DRG neurons (Fig. 2, Table 1).

DRG neurons were double-labeled to correlate Kv1 subunit expression with immunohistochemically defined cells. High-level expression of NaChs and Kv1.2 was mutually exclusive (Fig. 3*A*); small-diameter neurons contained a very high density of NaChs (red, arrowheads), whereas larger-diameter neurons expressed high levels of Kv1.2 (green). In stark contrast, small DRG neurons expressed high levels of both NaChs and Kv1.4 such that the staining patterns overlapped (yellow, Fig. 3*B*, arrowhead). Certain larger diameter cells expressed low NaCh and high Kv1.4 levels (Fig. 1, contra, arrowhead). VR-1, highly expressed in thermal nociceptors (24), most often correlated with high levels of NaCh staining (Fig. 3*C*, arrowhead), although some small-diameter neurons had only VR-1 (arrow) or NaCh (asterisk) immunoreactivity. Staining for NaCh subtype Nav1.8, present in peripheral nociceptors (25), overlapped with pan-NaCh staining of small-diameter DRG neurons (Fig. 2*D*). Taken together these results suggest that the majority of small-diameter DRG neurons

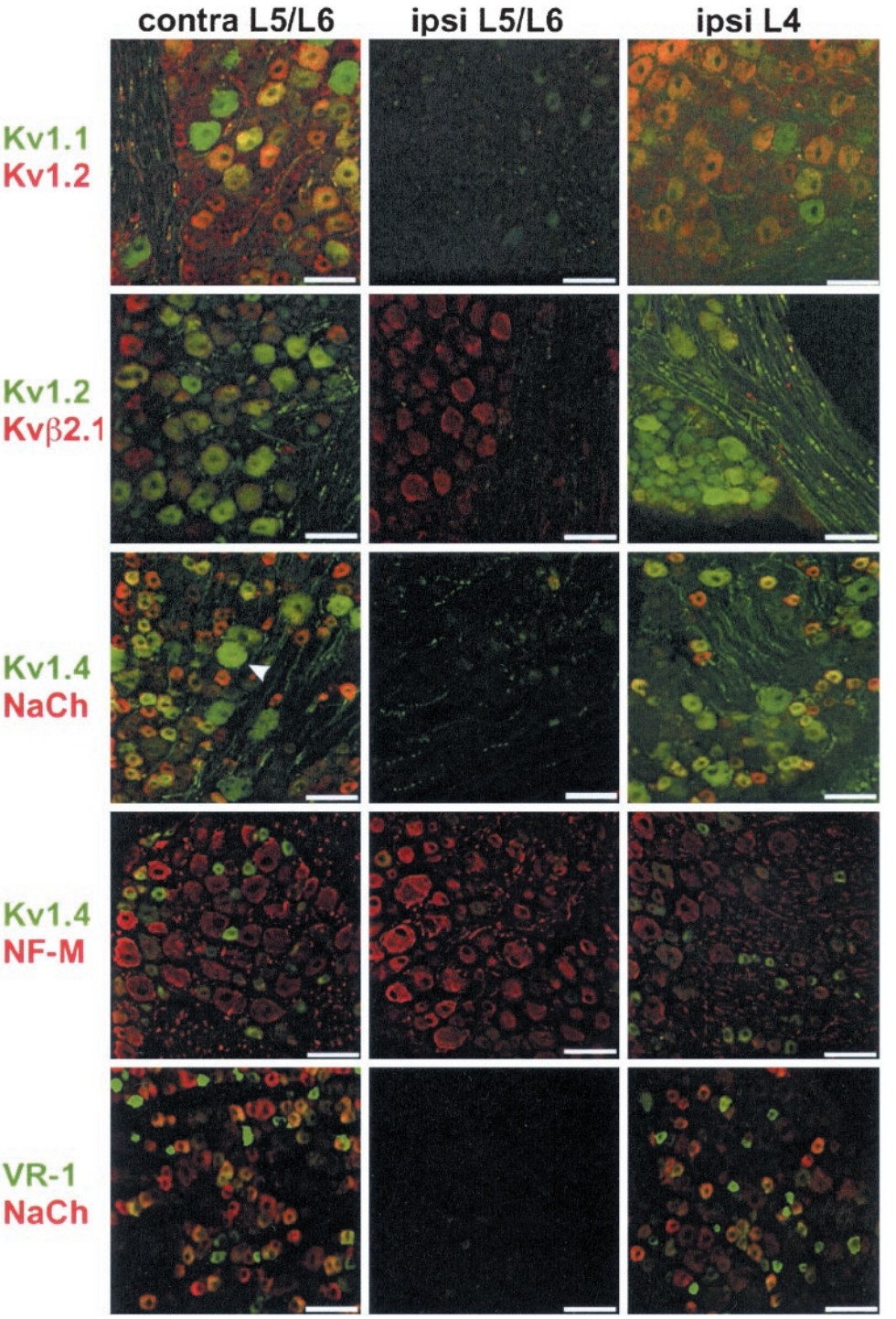

Fig. 1. Double-labeling of contralateral L5/L6, ipsilateral L4 (unligated), and ipsilateral L5/L6 (ligated) DRG, using antibodies against Kv1.1, Kv1.2, Kv1.4, Kvβ2.1, NaCh, VR-1, and NF-M. All tissue was processed simultaneously for each set of antibodies, and exposures for ipsilateral and contralateral sections were identical. (Scale bars, 100 μm.)

expressing Kv1.4, but not other Kv1 subunits, also express Nav1.8 and VR-1 and are likely nociceptors.

We quantified correlations between Kv1 subunit expression and these DRG markers (Table 1). For example, we found that 92% of Kv1.1-containing cells also expressed Kv1.2, and that large-diameter cells usually expressed Kv1.1, Kv1.2, and Kvβ2.1 (e.g., Fig. 1, contra), most likely as heteromultimeric channels as in rat brain (8), sciatic nerve (9), and spinal cord (21). In contrast, in those cells where NaChs were abundantly expressed, Kv1.1 and Kv1.2 subunits were rarely detected (2% and 11%, respectively; Figs. 1, contra, and 3*A*), whereas 88% of these pan-Nach-labeled neurons expressed Kv1.4 (Figs. 1, contra, and 3*B*). In support of these conclusions, triple-staining experiments showed that Kv1.1 (red) and Kv1.2 (blue) were usually found within the same cells (purple, Fig. 3*E*, arrow), and that Kv1.4 (green) was usually found in neurons not expressing Kv1.1 or

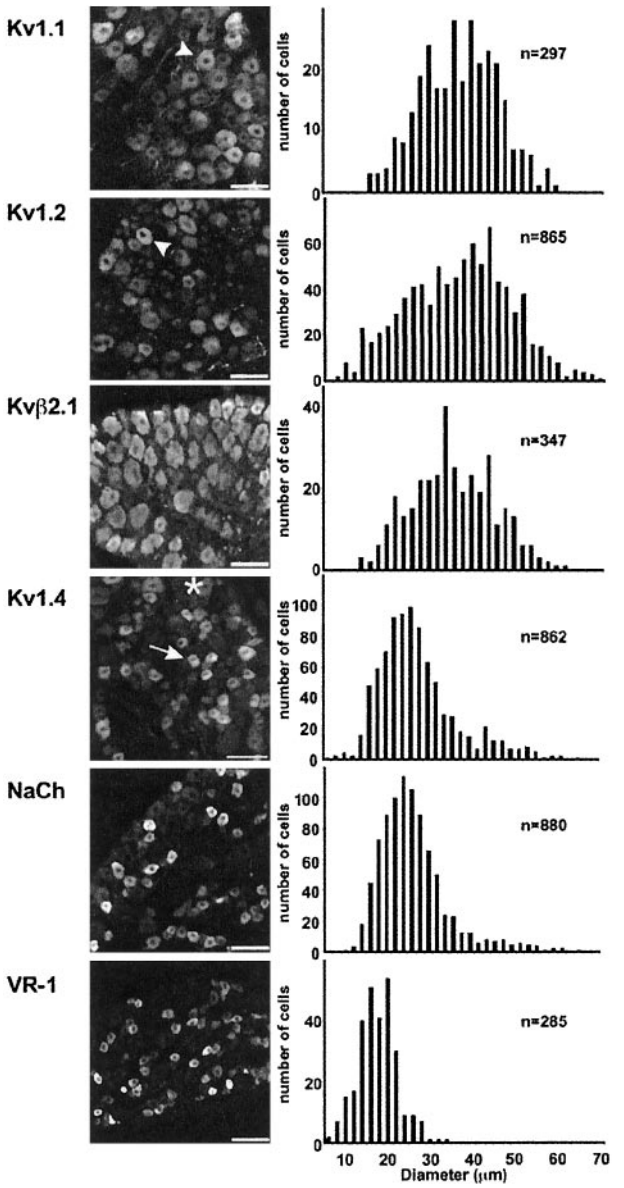

Fig. 2. Immunofluorescence staining of rat DRG and histograms showing diameters of cells labeled with ion channel-specific antibodies. (Scale bars, 100 μm.)

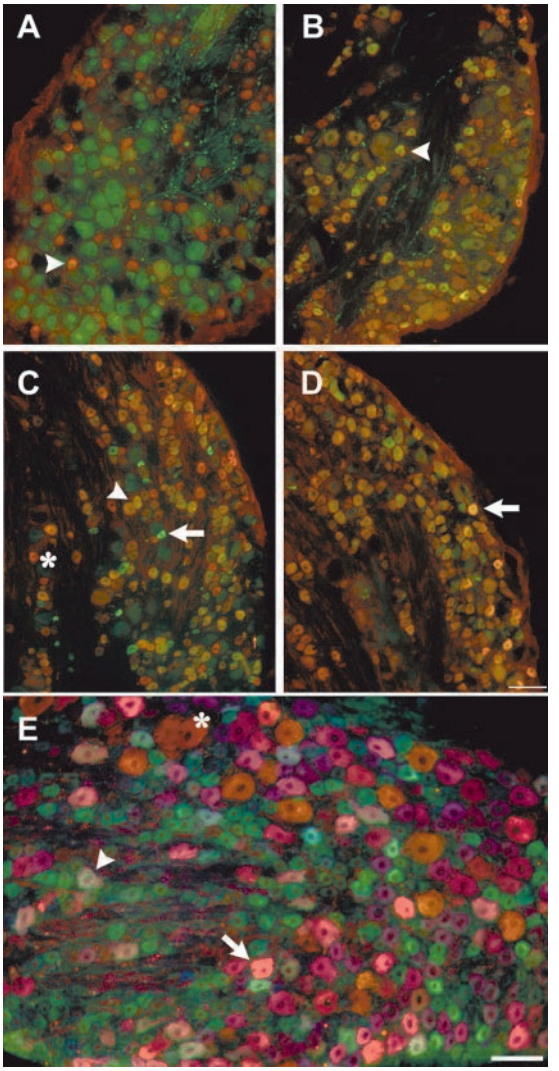

Fig. 3. Double- (*A–D*) and triple-labeling (*E*) of ion channels in DRG cryosections. (*A*) Kv1.2 (green) and pan-NaCh (red). Anti-pan-NaCh antibodies intensely labeled small-diameter cells (arrowheads), and weakly stained a few large-diameter cells that had overlapping Kv1.2 immunoreactivity (yellow). (*B*) Kv1.4 (green) and pan-NaCh (red). Most staining colocalized in small-diameter cells (arrowheads, yellow), but some larger-diameter cells were also labeled. (*C*) VR-1 (green) and pan-NaCh (red). Staining usually colocalized (arrowhead), but distinct subpopulations existed with either only VR-1 (arrow) or pan-NaCh (asterisk) immunoreactivity. (*D*) Nav1.8 (green) and pan-NaCh (red); overlap is yellow. (*E*) Kv1.1 (red), Kv1.2 (blue), and Kv1.4 (green). Most medium- and large-diameter cells had Kv1.1 and Kv1.2 staining that colocalized (arrow, violet). Some cells had immunoreactivity for all three subunits (arrowhead, white). A subpopulation of large diameter cells had primarily Kv1.1 immunoreactivity (asterisk, red). (Scale bars, 100 μm.)

Kv1.2. Because other Kv1 subunits were not detected in these small-diameter DRG neurons, these cells may assemble homotetrameric Kv1.4 channel complexes. However, in a small subset of cells Kv1.4 could form heteromultimeric complexes with Kv1.1 and Kv1.2 (arrowhead). Interestingly, in some of the largest-diameter DRG neurons Kv1.1 was observed in the absence of other Kv1 subunits, despite the fact that Kv1.1 homotetramers are usually not efficiently expressed on the cell surface (26).

Subcellular Localization of Kv1 Subunits in Axons of Sensory Neurons. To address the potential function of these Kv1 channels in sensory signal transduction, we determined the subcellular location of Kv subunits in sensory axons. Kv1.1, Kv1.2, and Kvβ2.1 colocalize at juxtaparanodal zones adjacent to nodes of Ranvier in myelinated axons in both peripheral and central nervous systems (7, 9, 19, 27). In dorsal spinal roots, whereas 67% (n = 256) of observed juxtaparanodes had only Kv1.1 and Kv1.2 (Fig. 4*A*, arrows), 29% were triple-labeled for Kv1.1/Kv1.2/Kv1.4 (Fig. 4*A*, arrowheads), and 4% were labeled for Kv1.1 and Kv1.4, but not Kv1.2 (not shown). Fig. 4*B* shows one such node of Ranvier (arrow) with nodal NaChs (green) and juxtaparanodal Kv1.4 (red). Juxtaparanodes containing only Kv1.1, Kv1.2, or Kv1.4 alone, or with Kv1.2 and Kv1.4, were not observed. In contrast to sensory fibers associated with DRG, the majority of juxtaparanodal Kv channels in motor ventral roots stained for Kv1.1 and Kv1.2 (Fig. 4*C*, arrows), and triple-labeling showed that Kv1.4 was not detected at the vast majority of juxtaparanodes (not shown). When ventral roots were double-labeled by

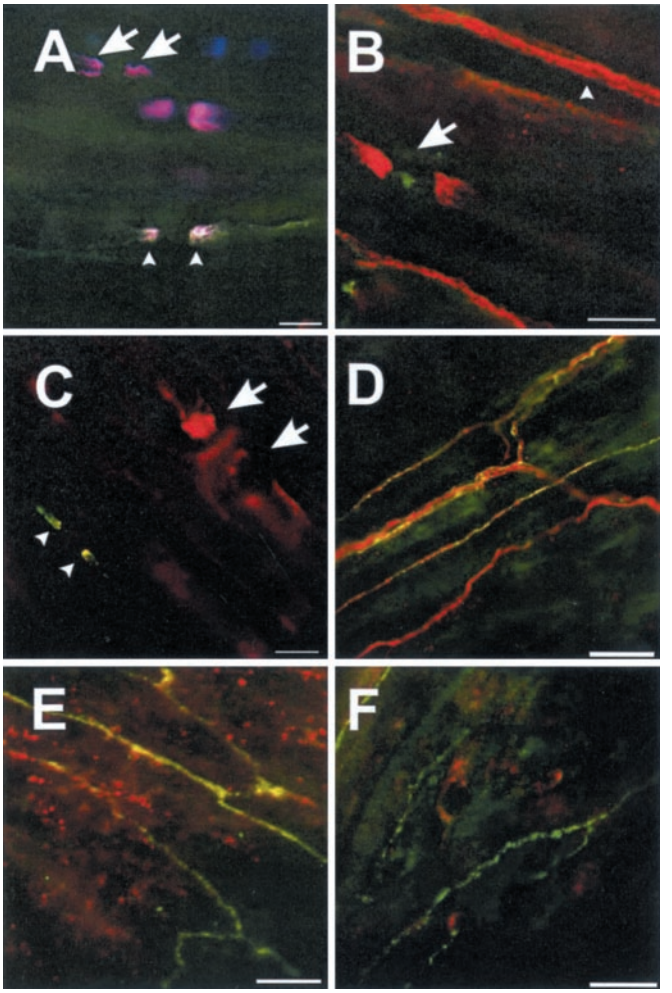

Fig. 4. Subcellular localization of Kv1 subunits in dorsal roots (*A*), ventral roots (*C*), Sciatic nerve (*B*), and unmyelinated axons in rat bladder (*D–F*). (*A*) Kv1.1 (red), Kv1.2 (blue), and Kv1.4 (green). Most juxtaparanodes had Kv1.1 and Kv1.2 (arrows), but some had all three Kv1 subunits colocalized (arrowheads). (*B*) Kv1.4 (red) and NaChs (green). Unmyelinated axons have a high density of Kv1.4 subunits (arrowhead). (*C*) Juxtaparanodes in ventral roots double-labeled with Kv1.4 and Kv1.2 (arrowheads, yellow) or Kv1.2 (arrows, red). (*D–F*) CGRP (green) and VR-1 (*E*), Kv1.4 (*F*), or Kv1.2 (*G*). (Scale bars, 10 μm.)

using antibodies against Kv1.2 and Kv1.4, only a small fraction (25/208 = 12%) of the observed juxtaparanodes had detectable Kv1.4. Importantly, this staining was detected only in the smallest-caliber axons with thin myelin sheaths (Fig. 4*C*, arrowheads), and Kv1.4 was never detected at juxtaparanodes from large-diameter ventral root fibers. Thus, when Kv1.4 is detected in myelinated axons, it is usually associated with sensory fibers.

Immunolabeling of unmyelinated axons was observed in rat sciatic nerve sections (Fig. 4*B*, arrowhead) and in rat bladder [many bladder afferents are C-fiber nociceptors (28, 29)]. Staining of the latter with antibodies against VR-1 (red) and CGRP (green), another marker of nociceptors, labeled bundles of suburothelial unmyelinated axons (Fig. 4*D*; overlap is yellow). CGRP and Kv1.4 immunoreactivity also overlapped in bladder afferents (Fig. 4*E*, yellow), whereas Kv1.2 staining was not detected in CGRP-labeled bladder axons (Fig. 4*F*). Thus, Kv1.4 channels are located in unmyelinated nociceptive axons in bladder and sciatic nerve, ideally positioned to modulate axonal conduction.

Discussion

Kv Channel Expression in Nerve Injury. Changes in ion channel expression, localization, or biophysical properties may underlie the onset of neuropathic pain following nerve injury, axotomy, or chronic inflammation. Application of hyperalgesic agents increases tetrodotoxin-resistant Na^+ currents in nociceptors (30) and axotomy results in up-regulation of Nav1.3 and down-regulation of Nav1.8 and Nav1.9 (30, 31). In contrast, Nav1.8 antisense treatment following nerve and tissue injury significantly attenuated hyperalgesia, suggesting a prominent role for this NaCh in certain models of chronic pain (32). We have shown that Kv channels are down-regulated dramatically in one model of neuropathic pain, which should result in a hyperexcitable state. Indeed, chronic bladder inflammation leads to a significant reduction in the A-type currents and nociceptor hyperexcitability (33).

Kv Channels in Large-Diameter DRG Neurons. Large-diameter DRG neurons (42–52 μm in diameter) express a prominent DTX-sensitive sustained or delayed rectifier-type Kv current (13) whose kinetic and pharmacological properties are consistent with high-level expression of Kv1.1/Kv1.2/Kvβ2.1 in similar-size DRG neurons, and in large-caliber myelinated axons. Large-diameter cutaneous afferent DRG neurons identified by *in vivo* retrograde labeling exhibited three distinct DTX-sensitive Kv currents, two sustained or slowly inactivating delayed rectifier-type currents, and a rapidly inactivating A-type current (16). The sustained current most probably corresponds to Kv1.1/Kv1.2/Kvβ2.1 channels seen in juxtaparanodes of many myelinated axons (9, 20). The slowly and rapidly inactivating Kv currents likely correspond to different heteromeric combinations of Kv1.1/Kv1.2/Kv1.4/Kvβ2.1 and Kv1.1/Kv1.4/Kvβ2.1. These combinations are expressed less frequently in large-diameter cells and at juxtaparanodes of some myelinated dorsal root axons representing the first description of juxtaparanodal Kv1.4 (8, 9).

Kv Channels in Small-Diameter DRG Neurons. Most Kv1.4-positive cells do not detectably express other Kv1 subunits, suggesting that Kv1.4 may form homotetrameric Kv channels in these cells. Small-diameter (18–30 μm) DRG neurons predominantly express a DTX-insensitive transient or A-type K^+ current whose properties correspond well with those expected for homotetrameric Kv1.4 channels, and 53% of these small-diameter cells are capsaicin-sensitive (13), a value nearly identical to that calculated from Table 1 for pan-Nach-labeled cells expressing both Kv1.4 and VR-1. Three transient Kv currents have been described in small diameter DRG neurons, two of which were found in neurons sensitive to capsaicin (34). Moreover, bladder nociceptive afferents express, in addition to TTX-insensitive NaChs and capsaicin receptors, a Kv1.4-like rapidly inactivating A-type current that contributes to the suppression of neuronal excitability (15). Chronic bladder inflammation increases the excitability of C fiber bladder afferent neurons through suppression of these A-type Kv channels (33), which together with data presented here suggest that Kv1.4 is a major determinant of C fiber excitability. It should be noted that Kv4.2 subunits also form DTX-insensitive A-type currents, and Kv4.2 plays an important role in determining the excitability of superior cervical ganglion cells (35). However, Kv4.2 is generally dendritic, whereas Kv1.4 is axonal (10, 12, 36). It should also be noted that although mice lacking Kv1.1 expression exhibit hyperalgesia (37), our data suggest that this may be due to central rather than peripheral effects.

That homotetrameric Kv1.4 channels may contribute directly to regulating conduction in C fibers is of particular importance

when considering pharmacological treatment of pain. An alternative to reducing nociceptor excitability through blockade of action potential depolarization, as with NaCh antagonists, may lie in enhancing or prolonging activity of Kv1.4. This might be accomplished by interfering with the "ball and chain" N-type inactivation that among Kv1 subunits is unique to Kv1.4. Moreover, neuronal homotetrameric Kv1.4 channels are unusual, because in most other neurons Kv1.4 exists primarily in heteromultimeric complexes (8, 11, 38, 39). Thus, an agonist specific for Kv1.4 homotetrameric channels might be expected to exhibit selectivity for small-diameter (predominantly nociceptive) sensory neurons.

We thank Dr. Louis Manganas for providing transfected COS-1 cell lysates, Dr. Gail Mandel for critical reading of the manuscript, and Chris LaBianca for technical assistance. Supported by National Institutes of Health Grants NS34383 and NS10906, and by Spinal Cord Research Foundation Grant 2040.

1. McCleskey, E. W. & Gold, M. S. (1999) *Annu. Rev. Physiol.* **61,** 835–856.
2. Isacoff, E. Y., Jan, Y. N. & Jan, L. Y. (1990) *Nature (London)* **345,** 530–534.
3. Ruppersberg, J. P., Schroter, K. H., Sakmann, B., Stocker, M., Sewing, S. & Pongs, O. (1990) *Nature (London)* **345,** 535–537.
4. Jan, L. Y. & Jan, Y. N. (1997) *Annu. Rev. Neurosci.* **20,** 91–123.
5. Rettig, J., Heinemann, S. H., Wunder, F., Lorra, C., Parcej, D. N., Dolly, J. O. & Pongs, O. (1994) *Nature (London)* **369,** 289–294.
6. Trimmer, J. S. (1998) *Curr. Opin. Neurobiol.* **8,** 370–374.
7. Wang, H., Kunkel, D. D., Martin, T. M., Schwartzkroin, P. A. & Tempel, B. L. (1993) *Nature (London)* **365,** 75–79.
8. Rhodes, K. J., Strassle, B. W., Monaghan, M. M., Bekele-Arcuri, Z., Matos, M. F. & Trimmer, J. S. (1997) *J. Neurosci.* **17,** 8246–8258.
9. Rasband, M. N., Trimmer, J. S., Schwarz, T. L., Levinson, S. R., Ellisman, M. H., Schachner, M. & Shrager, P. (1998) *J. Neurosci.* **18,** 36–47.
10. Sheng, M., Tsaur, M. L., Jan, Y. N. & Jan, L. Y. (1992) *Neuron* **9,** 271–284.
11. Rhodes, K. J., Keilbaugh, S. A., Barrezueta, N. X., Lopez, K. L. & Trimmer, J. S. (1995) *J. Neurosci.* **15,** 5360–5371.
12. Cooper, E. C., Milroy, A., Jan, Y. N., Jan, L. Y. & Lowenstein, D. H. (1998) *J. Neurosci.* **18,** 965–974.
13. Pearce, R. J. & Duchen, M. R. (1994) *Neuroscience* **63,** 1041–1056.
14. Gold, M. S., Shuster, M. J. & Levine, J. D. (1996) *J. Neurophysiol.* **75,** 2629–2646.
15. Yoshimura, N., White, G., Weight, F. F. & de Groat, W. C. (1996) *J. Physiol. (London)* **494,** 1–16.
16. Everill, B., Rizzo, M. A. & Kocsis, J. D. (1998) *J. Neurophysiol.* **79,** 1814–1824.
17. Everill, B. & Kocsis, J. D. (2000) *Neuroscience* **100,** 417–422.
18. Bekele-Arcuri, Z., Matos, M. F., Manganas, L., Strassle, B. W., Monaghan, M. M., Rhodes, K. J. & Trimmer, J. S. (1996) *Neuropharmacology* **35,** 851–865.
19. Rhodes, K. J., Monaghan, M. M., Barrezueta, N. X., Nawoschik, S., Bekele-Arcuri, Z., Matos, M. F., Nakahira, K., Schechter, L. E. & Trimmer, J. S. (1996) *J. Neurosci.* **16,** 4846–4860.
20. Rasband, M. N., Peles, E., Trimmer, J. S., Levinson, S. R., Lux, S. E. & Shrager, P. (1999) *J. Neurosci.* **19,** 7516–7528.
21. Rasband, M. N. & Trimmer, J. S. (2001) *J. Comp. Neurol.* **429,** 166–176.
22. Kim, S. H. & Chung, J. M. (1992) *Pain* **50,** 355–363.
23. Gulbis, J. M., Mann, S. & MacKinnon, R. (1999) *Cell* **97,** 943–952.
24. Caterina, M. J., Schumacher, M. A., Tominaga, M., Rosen, T. A., Levine, J. D. & Julius, D. (1997) *Nature (London)* **389,** 816–824.
25. Akopian, A. N., Sivilotti, L. & Wood, J. N. (1996) *Nature (London)* **379,** 257–262.
26. Manganas, L. N. & Trimmer, J. S. (2000) *J. Biol. Chem.* **275,** 29685–29693.
27. Rasband, M. N., Trimmer, J. S., Peles, E., Levinson, S. R. & Shrager, P. (1999) *J. Neurocytol.* **28,** 319–331.
28. Yoshimura, N., Erdman, S. L., Snider, M. W. & de Groat, W. C. (1998) *Neuroscience* **83,** 633–643.
29. Shea, V. K., Cai, R., Crepps, B., Mason, J. L. & Perl, E. R. (2000) *J. Neurophysiol.* **84,** 1924–1933.
30. Waxman, S. G., Dib-Hajj, S., Cummins, T. R. & Black, J. A. (1999) *Proc. Natl. Acad. Sci. USA* **96,** 7635–7639.
31. Novakovic, S. D., Tzoumaka, E., McGivern, J. G., Haraguchi, M., Sangameswaran, L., Gogas, K. R., Eglen, R. M. & Hunter, J. C. (1998) *J. Neurosci.* **18,** 2174–2187.
32. Porreca, F., Lai, J., Bian, D., Wegert, S., Ossipov, M. H., Eglen, R. M., Kassotakis, L., Novakovic, S., Rabert, D. K., Sangameswaran, L. & Hunter, J. C. (1999) *Proc. Natl. Acad. Sci. USA* **96,** 7640–7644.
33. Yoshimura, N. & de Groat, W. C. (1999) *J. Neurosci.* **19,** 4644–4653.
34. Gold, M. S., Reichling, D. B., Shuster, M. J. & Levine, J. D. (1996) *Proc. Natl. Acad. Sci. USA* **93,** 1108–1112.
35. Malin, S. A. & Nerbonne, J. M. (2000) *J. Neurosci.* **20,** 5191–5199.
36. An, W. F., Bowlby, M. R., Betty, M., Cao, J., Ling, H. P., Mendoza, G., Hinson, J. W., Mattsson, K. I., Strassle, B. W., Trimmer, J. S. & Rhodes, K. J. (2000) *Nature (London)* **403,** 553–556.
37. Clark, J. D. & Tempel, B. L. (1998) *Neurosci. Lett.* **251,** 121–124.
38. Shamotienko, O. G., Parcej, D. N. & Dolly, J. O. (1997) *Biochemistry* **36,** 8195–8201.
39. Felix, J. P., Bugianesi, R. M., Schmalhofer, W. A., Borris, R., Goetz, M. A., Hensens, O. D., Bao, J. M., Kayser, F., Parsons, W. H., Rupprecht, K., *et al.* (1999) *Biochemistry* **38,** 4922–4930.